Publication IV

Mikko Merimaa, Thomas Lindvall, Ilkka Tittonen, and Erkki Ikonen. 2003. All-optical atomic clock based on coherent population trapping in ^{85}Rb. Journal of the Optical Society of America B, volume 20, number 2, pages 273-279.

© 2003 Optical Society of America (OSA)

Reprinted by permission of Optical Society of America.

All-optical atomic clock based on coherent population trapping in ^{85}Rb

Mikko Merimaa,* Thomas Lindvall, Ilkka Tittonen, and Erkki Ikonen

Helsinki University of Technology, Metrology Research Institute, P.O. Box 3000, FIN-02015 HUT, Finland

Received March 12, 2002; revised manuscript received August 19, 2002

An all-optical microwave frequency standard based on coherent population trapping (CPT) in ^{85}Rb is developed. The CPT resonances are detected by an ordinary edge-emitting diode laser in a simple optical setup. A buffer-gas mixture is carefully optimized to yield a narrow linewidth and a reduced temperature dependence of the resonance frequency. With the developed system we are able to measure ultranarrow optically induced hyperfine CPT resonances at <20 Hz, which is in good agreement with the linewidth calculated from experimental parameters. The frequency of an RF-signal generator has been stabilized to the CPT resonance between the two $m_F = 0$ magnetic sublevels. The relative frequency stability (square root of Allan variance) follows a slope of $3.5 \times 10^{-11}\ \tau^{-1/2}$ (1 s $< \tau <$ 2000 s). The best stability of 6.4×10^{-13} is reached at an integration time of $\tau = 2000$ s. This stability is sufficient for many high-precision applications. Frequency-shift measurements were made to evaluate the frequency dependencies on the operation parameters. © 2003 Optical Society of America

OCIS codes: 020.1670, 300.6260, 300.6320, 300.3700, 120.3930.

1. INTRODUCTION

Atomic frequency standards are used in applications where the highest frequency stability and accuracy are needed. A simple and compact all-optical atomic frequency standard based on coherent population trapping (CPT) was proposed by Cyr *et al.* in 1993.[1] Such an atomic frequency standard has potential applications in areas where an intermediate step between the Cs atomic clock and a crystal oscillator is desired. Advances in diode lasers have made such devices feasible,[2–4] and, if sufficient stability is achieved, these devices could be used, e.g., in global navigation and telecommunications applications.

In CPT, two laser modes interacting with an atomic three-level Λ system, described in Fig. 1, are coupled by the ground-state coherence and interfere destructively at two-photon resonance. As the decay rate of the ground-state coherence is small, the linewidth is narrow, and the resonance forms a high-precision frequency reference. In practice, the linewidth and the absolute frequency of the resonance are determined by the experimental parameters as discussed in Subsection 2.C. Since the discovery of coherent population trapping by Alzetta *et al.* in 1976,[5] the phenomenon has found many applications including, e.g., laser cooling of atoms,[6] magnetometry,[7] and lasing without inversion.[8] The phenomenon has been recently reviewed by Arimondo[9] and studied by Vanier *et al.*,[10] Wynands *et al.*,[11] and Hollberg *et al.*[2–4] with emphasis on metrological applications.

In this study, we investigate CPT resonances in ^{85}Rb using an edge-emitting diode laser equipped with an integrated microlens. With this type of laser, phase-coherent first-order sidebands can be generated directly with high efficiency by modulating the laser frequency via injection current. The rubidium Λ system is used in this study because laser diodes operating at the wavelength of the ^{85}Rb $5^2S_{1/2}$–$5^2P_{3/2}$ transition (D_2 line) are easily available and the modulation bandwidth of edge-emitting diode lasers covers the ground-state hyperfine splitting. The good noise properties of the lasers allow detection of ultranarrow CPT resonances <20 Hz, apparently the narrowest optically induced hyperfine CPT resonance ever measured, which is also in good agreement with the linewidth calculated from experimental parameters.

The achieved performance is similar to other CPT clocks[4] but does not quite reach the level of conventional laser-pumped rubidium frequency standards.[12,13] However, it is anticipated[14] that the theoretically higher signal-to-noise ratio and the absence of the microwave cavity will eventually lead to CPT clocks, which are superior in terms of frequency stability and size as compared with the conventional laser-pumped frequency standards. An additional advantage of a CPT clock is lower sensitivity to light shift, which can significantly limit the performance of the conventional laser-pumped frequency standards.[15]

2. ALL-OPTICAL ATOMIC CLOCK

A. Laser Source

As the transition between the hyperfine-split ground states of alkali metals is electric dipole forbidden and has a long lifetime, the relative linewidth of the transition is essentially determined by the coherent interaction time and the ground-state hyperfine splitting (CPT resonance frequency). Assuming nearly the same coherent interaction time for different alkali atoms, the best relative frequency stability is anticipated with an atom having as large ground-state hyperfine splitting as permitted by the laser-diode modulation bandwidth. When the ground-state hyperfine splittings of the alkali atoms[16] are compared, the ^{85}Rb atom with approximately 3.0357-GHz

 © 2003 Optical Society of America

hyperfine splitting is found to be optimal for the ordinary edge-emitting diode lasers, which have modulation bandwidths typically between 2 and 5 GHz.

The laser source used in this study is a commercial edge-emitting diode laser (Blue Sky Research PS026, $\lambda = 780$ nm), which is equipped with an integrated microlens. The optical feedback from the closely mounted microlens ensures single-mode operation even under heavy current modulation. The microlens also improves the beam geometry and the frequency tunability of the laser: The oscillating modes can be selected by adjusting the distance between the microlens and laser diode. As the diode laser has a modulation bandwidth in excess of 3 GHz, it is suitable for spectroscopy of the Λ systems in the ^{85}Rb $5^2S_{1/2}$–$5^2P_{3/2}$ transition at 780.24 nm.

Edge-emitting diode lasers have intrinsically low-intensity noise, which is beneficial, as noise at the detection frequency essentially determines the signal-to-noise ratio of the measurement. The measured relative intensity noise of the laser used in this study is less than -135 dB/Hz around the measurement frequency (300 Hz), and the side-mode suppression ratio of the laser is >35 dB.

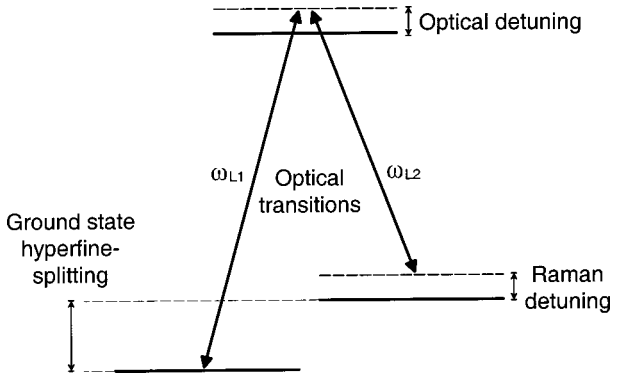

Fig. 1. Three-level Λ system. The two laser modes coupling the ground states to the common upper state are designated by ω_{L1} and ω_{L2}.

As the two laser modes used for CPT are generated from the same laser source through frequency modulation, the frequency noise of the fields is nearly perfectly correlated and has no effect on the relaxation rate of the ground-state coherence.[9] However, even though the frequency noise of the laser has no direct effect on CPT, the frequency noise can be converted to intensity noise in the resonance[17] and thus deteriorate the signal-to-noise ratio of detection. In this case, the frequency noise is determined by the properties of the laser diode, as the optical feedback from the microlens is too weak to reduce the linewidth of the laser diode. Fortunately, the high output power of the laser diode (of the order of 20 mW) and the properties of the laser cavity yield a relatively narrow linewidth of ~2 MHz.

B. Experimental Setup

The experimental setup used in this study is schematically shown in Fig. 2. The clock part of the optical setup consists of a rubidium cell, polarization and beam expansion optics, and a photodetector. The rubidium cell (length 50 mm, diameter 25 mm) is placed inside a magnetic shield together with a solenoid that is used to generate a 6-μT magnetic field to lift the Zeeman degeneracy of the hyperfine states. A long, 130-mm solenoid has been used to ensure the homogeneity of the magnetic field inside the cell. The variation of the longitudinal field strength is calculated to be $<1\%$, and the transversal field is calculated to be $<1\%$ of the longitudinal field. A nearly uniform beam-intensity profile is generated with a beam expander, which filters out the edges of the beam. To avoid saturation broadening of the CPT resonance, the intensity is further decreased with neutral-density filters to <10 μW/cm^2, which is close to the coherence saturation intensity given in Ref. 11 for cesium. As both laser modes originate from the same frequency-modulated laser diode, the modes are in the same polarization state. Since circular polarization gives a stronger signal in the

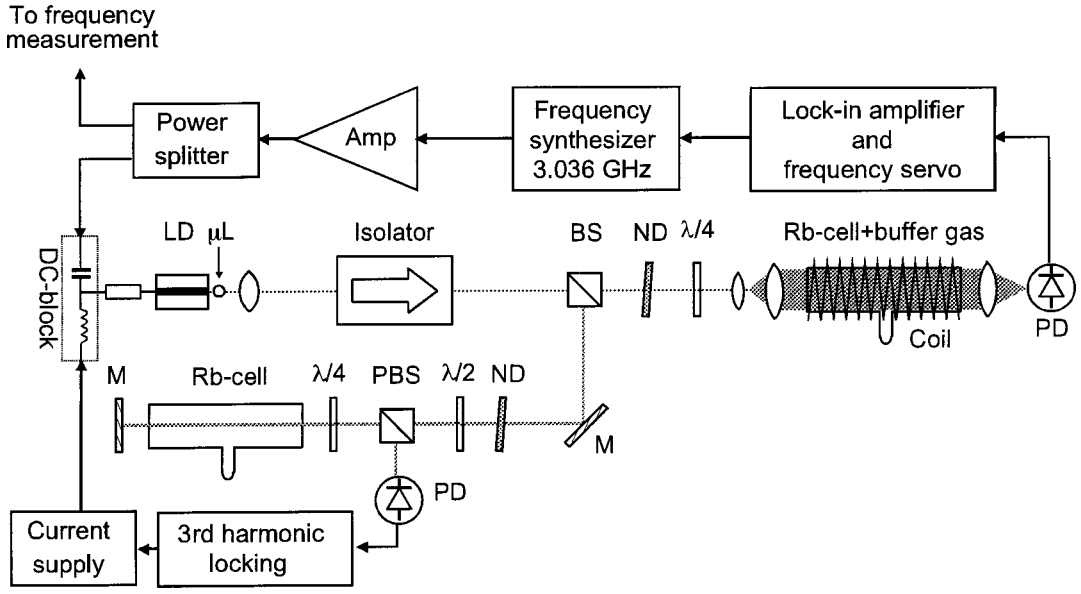

Fig. 2. Experimental setup: LD, laser diode; μL, microlens; $\lambda/2$, half-wave plate; $\lambda/4$, quarter-wave plate; ND, neutral-density filter; M, mirror; PBS, polarizing beam splitter; BS, beam splitter; and PD, photodetector.

presence of buffer gas,[18] a quarter-wave plate is placed into the setup. A lens is used to collect the light onto a large-area, high-quantum-yield p-i-n photodiode.

The electronic part of the setup is essentially a combination of a lock-in amplifier, a frequency servo, and an rf-signal generator. A low-noise signal generator (Agilent E4426B) is used to generate the 3.0357-GHz modulation frequency from a 10-MHz high-precision crystal oscillator, and the signal is further amplified to get a red sideband having 30% of the carrier power. A digital lock-in amplifier is used to detect the CPT resonance and to provide an error signal for frequency-locking electronics.

A laser frequency-stabilization scheme similar to the one described in Ref. 19 is used to lock the laser (carrier) frequency to the crossover component between the hyperfine components $F = 2 \rightarrow F' = 1$ and 2 of the D_2 line. This crossover component is used because it gives the strongest signal and partially compensates for the −130-MHz pressure shift[20] caused by the buffer gas. Due to the modulation-induced sidebands, the complete hyperfine structure of the excited state (with crossover components) is present, but it can be resolved with sufficient precision for frequency stabilization.

C. Buffer-Gas Selection

The maximum coherent interaction time, which limits the observable linewidth, is determined by the experimental parameters. If the laser modes are assumed to be completely phase coherent, the interaction time in rubidium vapor is limited by transit time or, with expanded beams, by wall collisions. A small contribution to the linewidth stems also from Rb–Rb collisions and Doppler broadening as the copropagating laser modes have slightly different frequencies.

Inert buffer gases, e.g., noble gases, can be used to increase the interaction time, as the diffusion of the rubidium atoms through the buffer gas increases the transit time and reduces wall collisions. In addition, the mean free path between collisions in buffer gas is shorter than the wavelength of the CPT resonance, and thus also the Doppler broadening is reduced (Dicke narrowing[21]), as discussed in Ref. 22.

The drawback of the buffer gas is the increased collisional broadening and the temperature-dependent pressure shift of the ground-state hyperfine splitting. The temperature dependence can be reduced with a mixture of argon and neon as a buffer gas, as argon and neon induce a negative and a positive temperature dependence, respectively. The optimum pressure ratio of $p_{\mathrm{Ar}}/p_{\mathrm{Ne}} \approx 0.87$ was calculated from the values given in Ref. 23 by use of the relative shifts being the same for the isotopes ^{85}Rb and ^{87}Rb.[24] The coherence decay rate is given by the equation[16]

$$\gamma_2 = C_1 p_0 \frac{D_{\mathrm{Ne}} D_{\mathrm{Ar}}}{D_{\mathrm{Ne}} p_{\mathrm{Ar}} + D_{\mathrm{Ar}} p_{\mathrm{Ne}}} + \frac{N_0}{p_0} (\bar{\nu}_{\mathrm{Rb\text{-}Ne}} \sigma_{\mathrm{Ne}} p_{\mathrm{Ne}} + \bar{\nu}_{\mathrm{Rb\text{-}Ar}} \sigma_{\mathrm{Ar}} p_{\mathrm{Ar}}) + C_2 N_{\mathrm{Rb}} \bar{\nu}_{\mathrm{Rb\text{-}Rb}} \sigma_{\mathrm{se}}, \quad (1)$$

where p_0 is the reference pressure (standard atmospheric pressure), N_0 is the reference density (buffer-gas density at reference pressure), D_{X} is the diffusion constant for rubidium in the gas X, $\bar{\nu}_{\mathrm{X-Y}}$ is the average relative velocity between atoms X and Y, σ_{Ar} and σ_{Ne} are the collisional dephasing cross sections, σ_{se} is the Rb–Rb spin-exchange collision cross section, and N_{Rb} is the density of rubidium. The constant C_1 is a geometrical factor depending on the shape and size of the cell, and the constant C_2 is the ratio between the spin-exchange decay rates of the coherences and the populations,[16]

$$C_2 = \frac{6I + 1}{8I + 4}, \quad (2)$$

where I is the nuclear spin of the alkali atom. With experimental parameters,[16,24] the minimization of the decay-rate equation yields the optimal pressures $p_{\mathrm{Ar}} \approx 16$ mbar and $p_{\mathrm{Ne}} \approx 19$ mbar. These values correspond to a theoretical CPT resonance linewidth of $\delta\nu = \gamma_2/\pi \approx 17$ Hz.

The calculated pressure shift of the CPT resonance is 2.2 kHz for the optimal pressures given above. The pressure shift is a major issue in a gas-cell-based atomic clock, as it is difficult to fill individual cells with highly precise buffer-gas pressures. This uncertainty in pressure, typically 1% in commercial cells, makes it necessary to characterize the intrinsic resonance frequency of each cell individually, which makes this type of an atomic clock a secondary frequency standard.

3. MEASUREMENT RESULTS

To avoid broadening of the CPT resonance by a weak ambient magnetic field, a magnetic field parallel to the laser beam is used to lift the Zeeman degeneracy of the hyperfine structure. This results in the formation of five open Λ systems when the $5^2S_{1/2}$–$5^2P_{3/2}$ transition of ^{85}Rb is used. The Λ system incorporating the $m_F = 0$ magnetic sublevels of the ground states $F = 2,3$ is used in all measurements, including the frequency stabilization of the RF-signal generator.

A. Coherent Population Trapping Resonances

The good noise properties of the laser source and the expanded beam allow detection of CPT resonances with low power densities and correspondingly small saturation broadening. As the passive relative frequency stability of the RF-signal generator is better than 5×10^{-11} (150 mHz) up to a 100-s integration time, low lock-in frequencies also can be used.

In the measurements we use typically a 1.3-μW/cm^2 intensity, and the 3.036-GHz sideband spacing is modulated at 325 Hz with a modulation index of 0.4. The modulation frequency of 325 Hz, between the sixth and the seventh harmonic of the line frequency, is used to minimize interference from the mains. With these values it is possible to obtain a reasonable signal-to-noise ratio in detection and a sufficient bandwidth of the feedback loop. The lock-in amplifier output is shown in Fig. 3 as a function of the Raman detuning.

To observe as narrow CPT resonances as possible, we used a very low intensity of 0.3 μW/cm^2. A low, 6-Hz modulation frequency was used (wavelength modulation), and the Lorenzian line shapes of Fig. 4 could be obtained through simple numerical integration of the lock-in am-

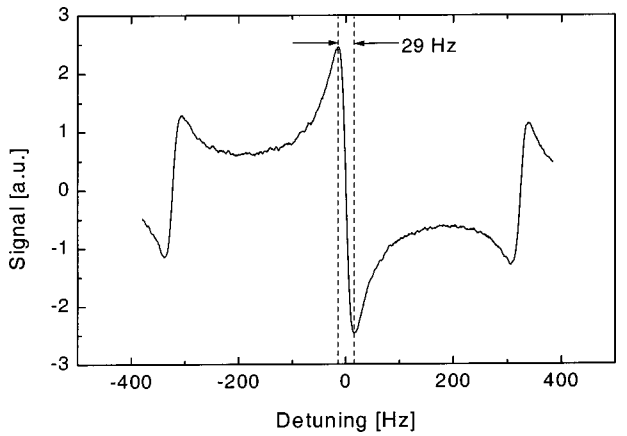

Fig. 3. Lock-in amplifier output when the frequency difference of the laser modes is swept over the CPT resonance frequency. This FM-spectroscopy signal was used in the frequency-stabilization experiments.

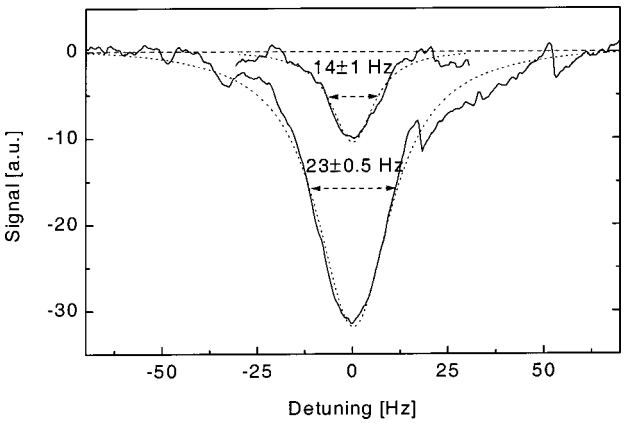

Fig. 4. Line shapes of CPT resonances measured with 0.3-μW/cm^2 intensity. Modulation amplitudes of 10 Hz (upper curve) and 19 Hz (lower curve) peak-to-peak were used in the measurement. The error estimates ± 0.5 Hz and ± 1 Hz refer to the uncertainty in fitting, the overall uncertainty being larger especially in the upper graph due to difficulties in determining the zero level.

plifier output signal. The curves in Fig. 4 show two examples of CPT resonances measured with 19-Hz and 10-Hz peak-to-peak modulation amplitudes, respectively. To estimate the FWHM of the measured CPT resonance, Lorenzian line shapes were fitted to the measurements. The linewidth given by the data measured with a 19-Hz peak-to-peak modulation amplitude is 23 Hz, which corresponds to a Q value of 1.3×10^8, comparable to Q values in cesium atomic clocks.[25] The poor signal-to-noise ratio of the measurement with 10-Hz peak-to-peak modulation amplitude complicates the determination of the zero level and correspondingly the evaluation of the linewidth. However, the linewidth of the optically induced hyperfine CPT resonance can be seen to be clearly below 20 Hz (Q value of 1.5×10^8), which is in good agreement with the theoretical estimation of $\sim$17 Hz.

B. Frequency Shifts

To evaluate the performance of the system as a frequency standard, the frequency dependencies on the operation parameters were measured. With optical detection and a gas-cell absorber, the observed frequency of an atomic resonance typically depends on the pressure in the cell, the temperature of the cell, the incident light intensity, and external fields.

1. Light Shift

In Ref. 26 it is assumed that in a true three-level Λ system, the nonabsorbing CPT resonance is not sensitive to the light shift even in the case of unequal Rabi frequencies. A more careful study of the solutions of the optical Bloch equations, still using the assumptions of Ref. 26, shows that the CPT resonance frequency is slightly affected by the light shift when the Rabi frequencies are not equal. To increase the accuracy of the light-shift calculations, OBE could be modified to take into account, e.g., the actual decay-rate ratio, which also slightly affects the CPT resonance frequency.

Unfortunately, the actual situation in rubidium transitions is more complicated than what is assumed in Ref. 26. The hyperfine structure of the $S_{1/2}$–$P_{3/2}$ transition of rubidium allows two excited states, $F' = 2$ and 3, for the Λ system. Also the single-photon transitions to $F' = 1$ or 4 contribute to the total light shift.[27,28] Accordingly, in our experiment the unused first-order blue sideband can have a nonnegligible effect to the light shift and should be taken into account. The situation is further complicated by the buffer gas, which is difficult to take into account in the optical Bloch equations.

The large number of contributing factors makes the calculation of the light shift difficult, and thus in this study the light shift is studied only experimentally to assess its effect on the frequency stability. Figure 5 shows the measured CPT resonance-frequency shift as a function of the total intensity for an intensity ratio of 0.3. The measured slope is approximately 0.3 Hz/μW/cm^2, which gives reasonably small relative sensitivity to intensity changes when a low, 2.3-μW/cm^2 intensity is used. The measured CPT resonance-frequency dependence on the intensity ratio of the laser modes is also shown in Fig. 6.

As the light shift depends on the optical detuning, the observed CPT resonance frequency is dependent on the

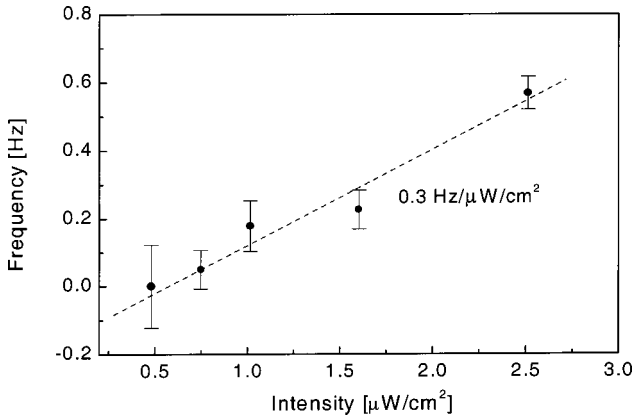

Fig. 5. Influence of the total intensity on the measured CPT resonance frequency. A linear model fitted to the measurement yields a 0.3-Hz/μW/cm^2 frequency dependence (dashed line) on the total intensity.

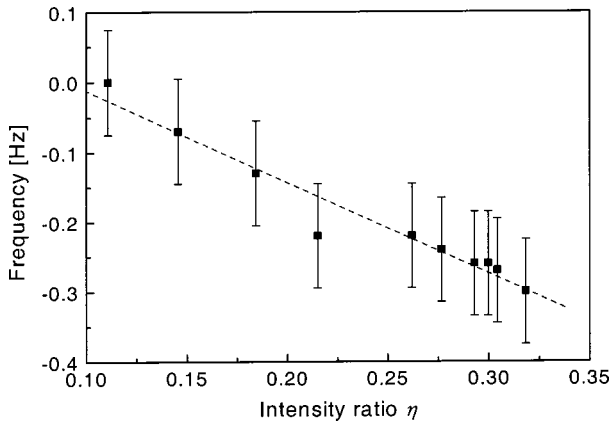

Fig. 6. Measured dependence of the CPT resonance frequency on the intensity ratio of laser modes. A linear model fitted to the measurement yields the frequency dependence $-1.3\ \mathrm{Hz} \times \eta$ (dashed line). The total intensity in this measurement was 2 μW/cm^2.

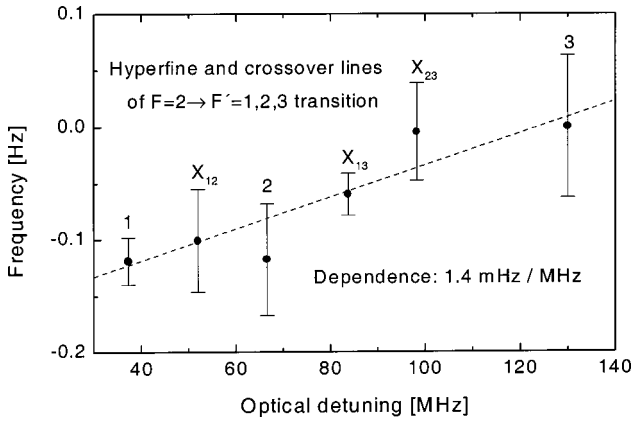

Fig. 7. RF frequency as a function of the laser frequency. The operating parameters are the same as typically used in frequency-stabilization experiments. A linear model fitted to the measurement yields a 1.4 mHz/MHz frequency dependence (dashed curve) on the laser frequency. The horizontal scale is the optical detuning from the −130-MHz pressure-shifted $F = 2 \rightarrow F' = 3$ transition.

optical frequency of the laser. Figure 7 shows the measured CPT resonance frequency as a function of the optical detuning from the pressure-shifted hyperfine component $F = 2 \rightarrow F' = 3$. Although a linear model is used to describe the measurement, this dependence should generally be taken to be nonlinear. The observed dependence is only 1.4 mHz/MHz, which is three orders of magnitude smaller than the values reported in Ref. 11 for cesium. The difference can be partially explained by the very low intensity used in this experiment, which further emphasizes the importance of applying low intensities in frequency-stabilization experiments.

2. Pressure and Temperature Shifts

The rubidium cell is thermally isolated, but the temperature is not actively stabilized, as the buffer-gas mixture is chosen to minimize the temperature dependence. The residual temperature dependence stems mainly from uncertainties in the measured temperature shifts[23] and can be estimated to be within ±100 mHz/K.

The buffer-gas-induced pressure shift causes the largest deviation of the CPT resonance from the unperturbed frequency, and the indeterminate magnitude of this shift requires individual calibration of the frequency produced by each cell. The measured shift of the CPT resonance frequency is ~2.56 kHz, which is in reasonable agreement with the calculated value of 2.2 kHz. Even though the cells used in this experiment are produced in the same batch, the observed frequency difference is 40 Hz, which is within the 1% pressure tolerance given by the manufacturer.

3. External Fields

Magnetic stray fields in the vicinity of the cell should be carefully minimized, as the nonlinear Zeeman shift has a relatively strong effect on the resonance frequency; see Fig. 8. To reduce the sensitivity to external magnetic fields, a low total longitudinal field of 6 μT is used to lift the Zeeman degeneracy. This value includes the magnetic field of the Earth, which couples to the cell through the optical windows and partially compensates the electrically induced field.

C. Frequency Stability

To measure the frequency stability of an RF-signal generator locked to the CPT resonance, another essentially similar setup was built. In this reference system the laser frequency is stabilized to the Doppler-broadened $F = 2 \rightarrow F' = 1,2,3$ transition with a Zeeman stabilization scheme similar to the one described in Ref. 29.

Figure 9 shows the measured relative frequency stability of an RF-signal generator locked to the CPT resonance as the square root of the Allan variance. The relative frequency stabilities of a high-quality crystal oscillator[30] and a commercial cesium atomic clock are given for reference. The relationship describing the relative frequency stability of the stabilized RF-signal generator is $3.5 \times 10^{-11}\ \tau^{-1/2}$ ($1\ \mathrm{s} < \tau < 2000\ \mathrm{s}$), and the best stability of 6.4×10^{-13} is reached at an integration time of $\tau = 2000$ s. This stability is sufficient for many high-

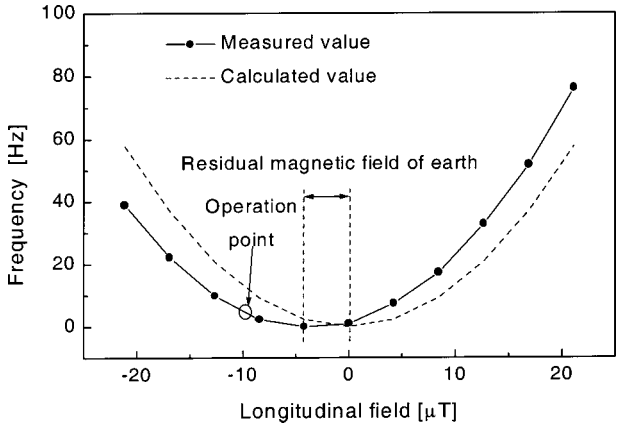

Fig. 8. Influence of the applied magnetic field on the measured frequency. As the optical setup is incidentally aligned approximately in the north-south direction, the magnetic field of Earth partially couples into the system through the optical windows. The calculated value is obtained from the Breit–Rabi formula.

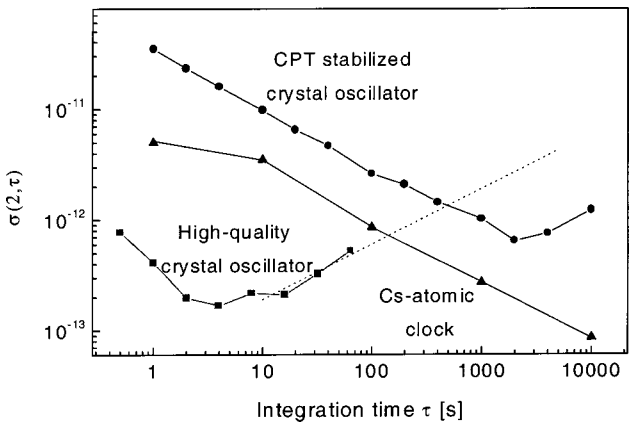

Fig. 9. Measured relative frequency stability (square root of Allan variance) of an RF-signal generator locked to the CPT resonance between the $m_F = 0$ magnetic sublevels (circles). For comparison, the relative frequency stability of a high-quality crystal oscillator (squares) and a commercial cesium atomic clock (triangles) are also given. The crystal oscillator data, with prediction to longer integration times, are taken from Ref. 30.

precision applications where, e.g., independence from the global positioning system signal is needed.

It is likely that the present performance is limited by temperature fluctuations of the rubidium cell, and, despite the temperature-compensated buffer gas, active temperature stabilization is needed to achieve better long-term frequency stability. In this particular design, the inadequate screening of external magnetic fields is also a factor limiting the long-term frequency stability. If flicker-floor levels $<10^{-13}$ (0.3 mHz) in the frequency stability are desired, other operation parameters will also have to be well stabilized. The relative intensity stability of the laser modes should be better than 10^{-4}, and an active intensity stabilization might be necessary. As the observed microwave frequency dependence on laser frequency is 1.4 mHz/MHz, the relative frequency stability of the laser must be better than 6×10^{-10}, which might be a limiting factor at long integration times if, e.g., linear absorption is used to stabilize the laser frequency.

As this type of an atomic clock is intended to serve as an intermediate step between crystal oscillators and cesium atomic clocks (or more advanced frequency standards), the additional complexity of operation parameter stabilization is not justified. The performance could be slightly improved without major modifications by use of a laser-mode intensity ratio closer to optimum or an even lower intensity, if permitted by signal-to-noise ratio and available space (cell diameter). There is also a possibility that a set of operation parameters minimizing the frequency dependencies could be found.[11]

4. CONCLUSIONS

We have demonstrated the applicability of ordinary edge-emitting diode lasers in the measurements of ^{85}Rb CPT resonances using a simple optical setup. The good noise properties of the system allow detection of ultranarrow CPT resonance <20 Hz, apparently the narrowest optically induced hyperfine CPT resonance ever measured and in good agreement with the linewidth calculated from experimental parameters. The observed linewidth corresponds to a Q value of 1.5×10^8, comparable to Q values in cesium atomic clocks. The system is also well suited for the future studies of low-intensity phenomena, like determination of the coherence saturation intensity.

The narrow CPT resonance has been used to lock an RF-signal generator to the Λ system between the $m_F = 0$ magnetic sublevels of ^{85}Rb transition $5^2S_{1/2}$–$5^2P_{3/2}$. The measured frequency stability slope of the system is $3.5 \times 10^{-11}\ \tau^{-1/2}$, and the best stability of 6.4×10^{-13} is reached at an integration time of 2000 s. This stability is sufficient for many high-precision applications. The frequency dependencies on operating parameters were experimentally studied to assess their effect on frequency stabilization. The relative sensitivity of the CPT resonance frequency to the operation parameters was found to be strongly dependent on the light intensity, which makes the use of low intensity desirable in the frequency standard application.

*E-mail: mikko.merimaa@hut.fi.

REFERENCES

1. N. Cyr, M. Têtu, and M. Breton, "All-optical microwave frequency standard: a proposal," IEEE Trans. Instrum. Meas. **42**, 640–649 (1993).
2. J. Kitching, S. Knappe, N. Vukiceviç, L. Hollberg, R. Wynands, and W. Weidmann, "A microwave frequency reference based on VCSEL-driven dark line resonances in Cs vapor," IEEE Trans. Instrum. Meas. **49**, 1313–1317 (2000).
3. J. Kitching, L. Hollberg, S. Knappe, and R. Wynands, "Compact atomic clock based on coherent population trapping," Electron. Lett. **37**, 1449–1451 (2001).
4. S. Knappe, R. Wynands, J. Kitching, H. G. Robinson, and L. Hollberg, "Characterization of coherent population-trapping resonances as atomic frequency references," J. Opt. Soc. Am. B **18**, 1545–1553 (2001).
5. G. Alzetta, A. Gozzini, L. Moi, and G. Orriols, "An experimental method for the observation of R.F. transitions and laser beat resonances in oriented Na vapour," Nuovo Cimento B **36**, 5–20 (1976).
6. A. Aspect, E. Arimondo, R. Kaiser, N. Vansteenkiste, and C. Cohen-Tannoudji, "Laser cooling below the one-photon recoil energy by velocity-selective coherent population trapping," Phys. Rev. Lett. **61**, 826–829 (1988).
7. M. O. Scully and M. Fleischnauer, "High-sensitivity magnetometer based on index-enhanced media," Phys. Rev. Lett. **69**, 1360–1363 (1992).
8. M. O. Scully, "From lasers and masers to phaseonium and phasers," Phys. Rep. **219**, 191–201 (1992).
9. E. Arimondo, "Coherent population trapping in laser spectroscopy," Prog. Opt. **35**, 257–354 (1996).
10. J. Vanier, A. Godone, and F. Levi, "Coherent population trapping in cesium: dark lines and coherent microwave emission," Phys. Rev. A **58**, 2345–2358 (1998).
11. R. Wynands and A. Nagel, "Precision spectroscopy with coherent dark states," Appl. Phys. B **68**, 1–25 (1999); erratum, Appl. Phys. B **70**, 315 (2000).
12. Y. Saburi, K. Koga, S. Kinugawa, T. Imamura, H. Suga, and Y. Ouchi, "Short-term stability of laser-pumped rubidium gas cell frequency standard," Electron. Lett. **30**, 633–635 (1994).
13. G. Mieti, J. Deng, F. L. Walls, D. A. Jennings, and R. E. Drullinger, "Laser-pumped rubidium frequency standards: new analysis and progress," IEEE J. Quantum Electron. **34**, 233–237 (1998).
14. J. Vanier, M. Levine, D. Janssen, and M. Delaney, "Coherent population trapping and intensity optical pumping: on

their use in atomic frequency standards" in *Proceedings of the Sixth Symposium on Frequency Standards and Metrology*, P. Gill, ed. (World Scientific, Singapore, 2002), pp. 155–166.
15. J. C. Camparo, "Reducing the light-shift in diode laser pumped rubidium atomic clock," in *Proceedings of the 1996 IEEE International Frequency Control Symposium* (Institute of Electrical and Electronics Engineers, Piscataway, N.J., 1996), pp. 988–992.
16. J. Vanier and C. Audoin, *The Quantum Physics of Atomic Frequency Standards* (Hilger, London, England, 1989).
17. J. Kitching, H. G. Robinson, L. Hollberg, S. Knappe, and R. Wynands, "Optical-pumping noise in laser-pumped, all-optical microwave frequency references," J. Opt. Soc. Am. B **18**, 1676–1683 (2001).
18. R. Wynands, A. Nagel, S. Brandt, D. Meschede, and A. Weis, "Selection rules and line strengths of Zeeman-split dark resonances," Phys. Rev. A **58**, 196–203 (1998).
19. H. Talvitie, M. Merimaa, and E. Ikonen, "Frequency stabilization of a diode laser to Doppler-free spectrum of molecular iodine at 633 nm," Opt. Commun. **152**, 182–188 (1998).
20. Ch. Ottinger, R. Scheps, G. W. York, and A. Gallagher, "Broadening of the Rb resonance lines by the noble gases," Phys. Rev. A **11**, 1815–1828 (1975).
21. R. H. Dicke, "The effect of collisions upon the Doppler width of spectral lines," Phys. Rev. **89**, 472–473 (1953).
22. M. Erhard, S. Nußmann, and H. Helm, "Power broadening and Doppler effects of coherent dark resonances in Rb," Phys. Rev. A **62**, 061802(R)1–4 (2000).
23. P. L. Bender, E. C. Beaty, and A. R. Chi, "Optical detection of narrow Rb^{87} hyperfine absorption lines," Phys. Rev. Lett. **1**, 311–313 (1958).
24. J. Vanier, J.-F. Simard, and J.-S. Boulanger, "Relaxation and frequency shifts in the ground state of Rb^{85}," Phys. Rev. A **9**, 1031–1040 (1974).
25. D. B. Sullivan, J. C. Bergquist, J. J. Bollinger, R. E. Drullinger, W. M. Itano, S. R. Jeffers, W. D. Lee, D. Meekhof, T. E. Parker, F. L. Walls, and J. D. Wineland, "Primary atomic frequency standards at NIST," J. Res. Natl. Inst. Stand. Technol. **106**, 47–63 (2001).
26. G. Orriols, "Nonabsorption resonances by nonlinear coherent effects in a three-level system," Nuovo Cimento B **53**, 1–23 (1979).
27. M. Arditi and J.-L. Picqué, "Precision measurements of light shifts induced by a narrow GaAs laser in the 0-0 ^{133}Cs hyperfine transition," J. Phys. B **8**, L331–L335 (1975).
28. F. Levi, A. Godone, and J. Vanier, "The light shift effect in the coherent population trapping cesium maser," IEEE Trans. Ultrason. Ferroelect. Freq. Control **47**, 466–470 (2000).
29. K. L. Corvin, Z.-T. Lu, C. F. Hand, R. J. Epstein, and C. E. Wieman, "Frequency stabilized diode laser with the Zeeman shift in an atomic vapor," Appl. Opt. **37**, 3295–3298 (1998).
30. M. B. Bloch, J. C. Ho, C. S. Stone, A. Syed, and F. L. Walls, "Stability of high-quality quartz crystal oscillators: an update," in *Proceedings of the 43rd Annual Symposium Frequency Control* (Institute of Electrical and Electronics Engineers, Piscataway, N.J., 1989), pp. 80–84.